Chem. Senses 36: 169–176, 2011

doi:10.1093/chemse/bjq107
Advance Access publication October 18, 2010

Different BOLD Responses to Intragastric Load of L-glutamate and Inosine Monophosphate in Conscious Rats

Tomokazu Tsurugizawa, Akira Uematsu, Hisayuki Uneyama and Kunio Torii

Institute of Life Sciences, Ajinomoto Co., Inc., Suzuki-cho 1-1, Kawasaki-ku, Kawasaki 210-8601, Japan

Correspondence to be sent to: Kunio Torii, Institute of Life Sciences, Ajinomoto Co., Inc., Suzuki-cho 1-1, Kawasaki-ku, Kawasaki, 210-8601, Japan. e-mail: kunio_torii@ajinomoto.com

Accepted September 13, 2010

Abstract

In this study, we compared the blood oxygen level–dependent (BOLD) signal changes between intragastric load of monosodium L-glutamate (MSG) and inosine monophosphate (IMP), which elicit the umami taste. An intragastric load of 30 mM IMP or 60 mM MSG induced a BOLD signal increase in several brain regions, including the nucleus of the solitary tract (NTS), lateral hypothalamus (LH), and insular cortex. Only MSG increased the BOLD signal in the amygdala (AMG). The time course of the BOLD signal changes in the NTS and the LH in the IMP group was different from that of the MSG group. We further compared the brain regions correlated with the BOLD signal change in the NTS between MSG and IMP groups. The BOLD responses in the hippocampus and the orbital cortex were associated with activation of the NTS in both MSG and IMP groups, but the association in the AMG and the pyriform was only in MSG group. These results indicate that gut stimulation with MSG and IMP evoked BOLD responses in distinct regions with different temporal patterns and that the mechanism of perception of L-glutamate and IMP in the gastrointestinal tract differed from that in the taste-sensing system.

Key words: fMRI, L-glutamate, inosine monophosphate, nucleus of the solitary tract, rat, umami

Introduction

L-glutamate (Glu) and inosine monophosphate (IMP) stimulate the gustatory cells in taste buds by interacting with taste receptors such as the T1R1 and T1R3 heterodimers, and they elicit umami taste in humans and rodents (Ninomiya et al. 2000; Nelson et al. 2002). Interestingly, umami substances display synergism: for instance, the combination of monosodium L-glutamate (MSG) and IMP augments the umami taste through the T1R1 and T1R3 receptors in the oral cavity (Zhang et al. 2008). Despite advanced studies of chemoreception in the oral cavity, the pathway that transmits information about ingested IMP from the gastrointestinal (GI) tract to the brain remains unclear.

In the GI tract, Glu and IMP are key molecules in cell metabolism. Metabolites from Glu are used as an intermediate in the citric acid cycle in the body. Glutamate also plays an important role in the body's disposal of excess or waste nitrogen. In contrast, IMP is the first nucleotide formed during the synthesis of purines and is found in nucleic acids and adenosine triphosphate, which are used to store chemical energy in muscle and other tissues (Watterson et al. 2007). Recent studies have revealed the existence of taste-sensing systems for Glu (e.g., T1Rs and α-gustducin) in the GI epithelium as well as in the oral cavity (Bezencon et al. 2007) and shown the postingestive effects using the taste-signaling system KO mice (Ren et al. 2010). Electrophysiological studies have shown that an intragastric or an enteral load of MSG accelerates vagal activity (Niijima 1991, 2000). A recent behavioral study revealed that MSG accelerates the postingestive conditioned flavor preference in rats and that an abdominal vagotomy significantly reduces these effects, indicating that information about the ingested Glu is transmitted from the GI tract to the brain via the vagus nerve (Uematsu et al. 2010). Although electrophysiological and behavioral researchers have investigated the effects of Glu (Bachmanov et al. 2009; Toyomasu et al. 2010), a study examining the effects of IMP has not yet been performed.

One of the great advantages of functional magnetic resonance imaging (fMRI) is that we can simultaneously detect the brain regions that are activated by nutrient stimuli. Moreover, using the time course of blood oxygenation level–dependent (BOLD) signal changes, we can investigate the functional correlations between brain regions (Shyu et al.

2004). A previous study using this analytical approach revealed the functional connectivity of the dopaminergic or serotonergic systems during the intravenous infusion of drugs in rats (Schwarz et al. 2009). In our previous study, we presented the BOLD response following intragastric administration of MSG in conscious rats (Tsurugizawa et al. 2009); however, the BOLD response to an intragastric load of IMP has not yet been investigated. The purpose of the present study was to clarify the differences in the BOLD response between intragastric loads of 60 mM MSG and 30 mM IMP, which are the preferable concentrations (Yamamoto et al. 2009), in conscious rats. We further compared the brain regions that were associated with the nucleus of the solitary tract (NTS) because the NTS is the terminal of the vagus nerve innervating the GI tract.

Materials and methods

Animals and surgery

Measurements of the BOLD signal were performed using 14 male Wistar rats (9 weeks old at the start of surgery, Charles River Laboratories) in each group; MSG ($n = 8$) and IMP ($n = 6$). The rats were housed individually in wire mesh cages under controlled conditions of temperature (23 ± 0.5 °C) and 12:12 h light:dark cycle, with free access to food (CRF-1; Oriental Yeast) and water. All animal procedures in the present study were approved, and they followed institutional guidelines.

To facilitate awake MRI measurements, we performed cranioplastic surgery on the rats under pentobarbital anesthesia (50 mg/kg body weight, intraperitoneally), as previously described. Briefly, for intragastric cannulation, one end of a silicone tube was passed from the abdomen under the skin of the back and held on the head. Cranioplastic acrylic cement was applied to the skull with 2 holes molded on each side to serve as receptacles for the 4 glass fiber bars that would hold the rat's head fixed during the MRI session. The other end of the silicone tube was inserted into the gastric fundus and ligated with a silk thread. After surgery, the rats were allowed to recover for more than 1 week.

FMRI training

The acclimation method previously described was used (Tsurugizawa et al. 2010). The rats were trained for 5 days to allow them to adapt to the awake fMRI conditions. They were trained at the same time each day (10:00–17:00) to minimize the effects of circadian rhythm variations. During the first 3 days, a pseudo-MRI system consisting of a nonmagnet bore and a head positioner was used. At first, the rats were lightly anesthetized for a short period of time using 2% isoflurane. The rats were then immediately set into the head positioner by fixing 4 bars to the cranioplastic acrylic mount, and their bodies were gently restrained with elastic bands. To reduce possible stress induced by the scanning noise, we used earplugs on the rats throughout the experiment. The rats were then left in the pseudo-MRI apparatus for 30 min on the first day and 90 min on the second and third days after recovery from anesthesia. During the next 2 days, the rats were placed in an MRI system under the same conditions as those used for the MRI measurements. Throughout the training, heart rate and respiration rate were measured using an MR-compatible monitoring system (Model 1025; SA Instruments). We confirmed that the respiration and heart rates on the fifth day were normal.

FMRI procedure

All MRI measurements were performed during the dark period after the rats had been fasted for 12–15 h. The rats had previously been fitted with gastric cannulae and cranioplastic acrylic cement and were anesthetized for a short time with 2% isoflurane. The rats' heads were then immediately immobilized with the cranioplastic acrylic mount fitted with 4 glass fiber bars on a nonmagnetic stereotaxic apparatus. This technique allowed us to avoid the painful insertion of ear bars. We then initiated scanning. The studies utilized a Bruker Avance III system (Bruker BioSpin) with a 4.7 T/40 cm horizontal superconducting magnet equipped with gradient coils (73 mT/m, 26 cm diameter). BOLD fMRI data were obtained using a T_2^*-weighted multislice fast low-angle shot sequence with the following parameters: time of repetition = 15 s, echo time = 10 ms, flip angle = 30°, field of view = 35 × 35 mm, acquisition matrix = 64 × 64, slice thickness = 1.3 mm, and slice number = 17. Structural images were obtained by multislice rapid acquisition with a relaxation enhancement (RARE) sequence using the following parameters: time of repetition = 2500 ms, effective echo time = 60 ms, RARE factor = 8, acquisition matrix = 128 × 128 and 4 averages. Twenty minutes after scanning began, a 60 mM MSG (Ajinomoto Co., Inc.) or a 30 mM IMP (Ajinomoto Co., Inc.) solution was delivered into the stomach for 10 min via the implanted tube at a rate of 1 mL/min/kg body weight by means of a syringe pump (CVF-3200; Nihon Kohden) in order to reduce the effects of gastric expansion (Figure 1).

Data analysis

The SPM5 software (Welcome Trust Center for Neuroimaging) was used for preprocessing, including slice realignment, coregistration of the functional image to a structural brain image, and spatial normalization of the functional data. Before preprocessing, template images that were coregistered to the Paxinos and Watson rat brain atlas were obtained (Paxinos and Watson 1998). Image sets containing motion artifacts were discarded. Statistical analyses were conducted using a program written in MATLAB (Mathworks, Inc.), as previously described (Tsurugizawa et al. 2010). The brain regions showing significant BOLD changes were determined by applying boxcar functions. The "off" period of the boxcar function was the basal period, corresponding to the period

during the 10 min before the start of nutrient administration, and the ''on'' period was the period of potential activity, in which measurements were obtained for every 5 min after the start of nutrient administration, for a total of 4 periods (Figure 1). To exclude fluctuations in the control states between groups, we confirmed that there were no significant changes in the BOLD signal intensity during the 10-min period prior to drug administration both within and between groups, using 2-way repeated measures analysis of variance. The first-level (fixed effect) analysis was performed on the data from individual animals. In order to make inferences about the group data, second-level (random effect) analyses were conducted using the results of the first-level analysis. We also compared the BOLD signals between MSG and IMP groups in a group analysis. The areas that showed significant activation ($P < 0.01$, corrected for multiple comparisons using false discovery rate procedure) and had a cluster size greater than 49 pixels were analyzed to remove the small clusters.

For the time series analysis, voxel of interests (VOIs) were created using the MRIcroN software. We drew the VOIs according to the Paxinos and Watson rat brain atlas (Paxinos and Watson 1998). The time course of the changes in BOLD signals within a VOI was calculated as follows:

$$\%\ \text{changes in BOLD signal intensity} = \left(\frac{\text{BOLD signals within VOI}}{\text{Averaged BOLD signals within VOI in basal period}} - 1\right) \times 100,$$

where the basal period applies to the 10 min before infusion.

Correlation analysis

Maps of BOLD signal changes correlated across subjects with the BOLD signal changes in a reference brain region were calculated using a program written in MATLAB. We used the NTS VOI that was made from the Paxinos and Watson rat brain atlas (Paxinos and Watson 1998). In the first-level analysis of the correlation analysis, we used the same VOI through all subjects. We constructed a design matrix composed of a regressor that captured the mean signal within the VOI in each animal. The second-level analyses were conducted across subjects. The areas that showed significant activation ($P < 0.01$, corrected for multiple comparisons using false discovery rate procedure) and had a cluster size greater than 49 pixels were analyzed in order to construct the t-contrast images.

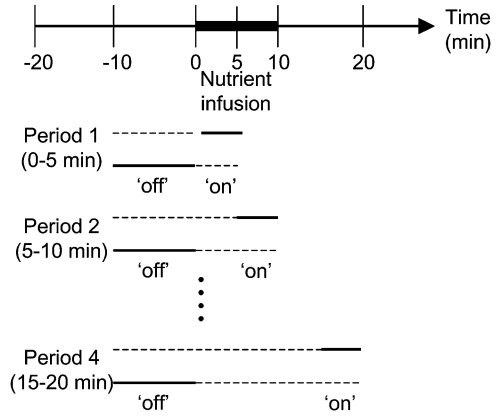

Figure 1 A diagram of the fMRI analysis. Functional data were obtained every 15 s for 40 min. The boxcar function is composed of "off" and "on" periods. The "off" period was defined as the 10 min before administration, and the "on" period was defined as every 5 min after the start of administration. There were a total of 4 "on" periods.

Results

BOLD signal increase by intragastric load of MSG or IMP

The *T*-map images induced by the administration of a 60 mM MSG or 30 mM IMP solution at periods 1, 2, 3, and 4 are shown in Figure 2. The *t* values and the periods when

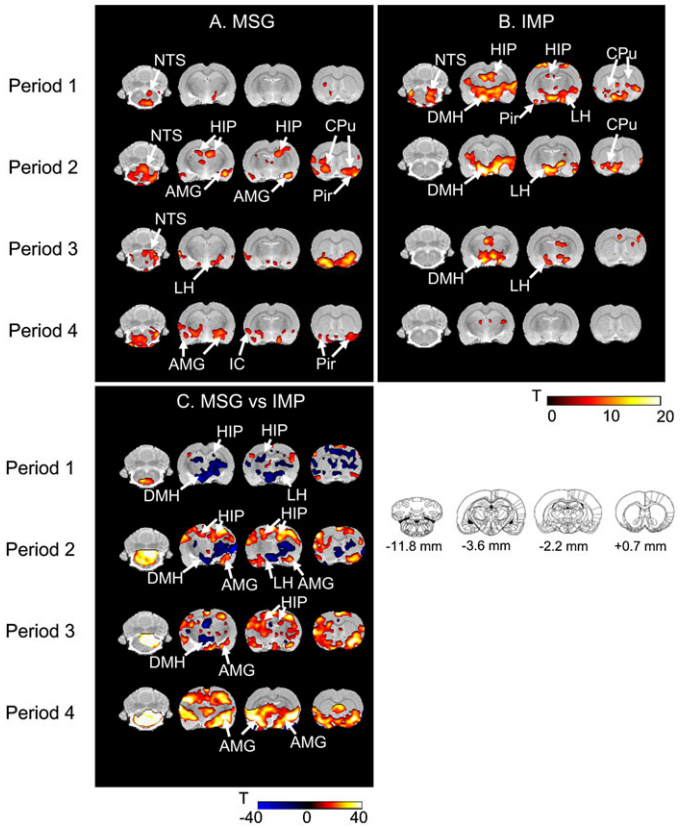

Figure 2 The areas of the rat brain responding to **(A)** 60 mM MSG or **(B)** 30 mM IMP solution in conscious rats at 0–5 min (period 1), 5–10 min (period 2), 10–15 min (period 3), and 15–20 min (period 4) after the start of the infusion. The *t* values show significant changes in the BOLD signal intensity compared with the preadministration period. **(C)** Comparisons between MSG and IMP groups. *t* Value shows the significant changes in BOLD signal intensity in MSG group compared with IMP group at the same time period. The lower right panel is the coronal figures of Paxinos Atlas at −12.2, −3.6, −2.2, and +0.7 mm from the bregma. Color bar, *t* value; AMG; CPu, caudate putamen; DMH, dorsomedial hypothalamus; HIP, hippocampus; IC, insular cortex; LH; NTS; Pir, piriform cortex.

the BOLD signals changed most significantly in each brain region are given in Table 1. MSG significantly increased the BOLD signals in several brain regions including the bilateral NTS, anterior cingulate cortex, infralimbic cortex, insular cortex, caudate putamen, amygdala (AMG), hippocampus, septum, hypothalamic areas, ventral/dorsal raphe nucleus, and locus ceruleus. IMP also induced a significant increase in the BOLD signal in several brain regions, including the bilateral anterior cingulate cortex, infralimbic cortex, caudate putamen, hippocampus, septum, hypothalamic areas, ventral/dorsal raphe nucleus, the left NTS, AMG, and insular cortex. Only MSG induced positive BOLD changes in the ventral pallidum, posterior part of the hypothalamus, lateral parabrachial nucleus, and locus ceruleus. IMP increased the BOLD signal in the ventroposteromedial thalamus and the arcuate nucleus, but MSG did not. The temporal pattern of the BOLD signal increases was also different. The BOLD signal changes in MSG group compared with IMP group show that, in period 4, the area of the BOLD signal increase in the MSG group was greater than that in the IMP group, whereas in period 1, the area of the IMP-induced BOLD increase was greater than that of the MSG-induced increase (Figure 2C).

Figure 3 shows the time course of the BOLD signal changes, averaged over 5-min periods, in the NTS, AMG, and lateral hypothalamus (LH), for both the MSG and the IMP groups. In the NTS, BOLD signal increased with a similar pattern in the MSG and IMP groups during the infusion period, but the patterns were different after the infusion period. Although the BOLD signal gradually

Table 1 Brain regions showing the most significant increases ($P < 0.01$, corrected) in the BOLD signal following the intragastric administration of an MSG or IMP solution

	MSG		IMP	
	period (min)	Maximum *t* value	period (min)	Maximum *t* value
Anterior cingulate cortex	15–20/15–20	10.9/10.99	15–20/15-20	7.71/7.54
Infralimbic cortex	10–15/10–15	7.72/6.39	10–15/10–15	9.19/10.96
Insular cortex	5–10/10–15	8.59/9.96	5–10/–	8.78/–
Caudate putamen	15–20/0–5	8.15/7.61	5–10/10–15	8.75/7.89
Amygdala	5–10/5–10	9.04/9.09	5–10/–	8.93/–
Piriform cortex	15–20/15–20	14.02/10.98	–/5–10	–/8.08
Hippocampus	10–15/5–10	9.52/7.72	5–10/5–10	7.66/7.81
Habenular nucleus	10–15/10–15	7.72/8.13	5–10/15–20	11.63/14.27
Septum	5–10/15–20	7.11/8.27	5–10/5–10	8.81/8.49
Ventral pallidum	15–20/15–20	11.35/12.3	–/–	–/–
Mamillary body	10–15/5–10	9.44/11.02	10–15/10–15	14.22/16.01
Mediodorsal thalamus	10–15/10–15	6.49/8.43	0–5/5–10	9.57/9.54
Ventroposteromedial thalamus	–/–	–/–	10–15/10–15	8.71/6.58
mPOA	15–20/15–20	6.78/7.33	15–20/10–15	6.76/11.06
Dorsomedial hypothalamus	–/5–10	–/7.81	15–20/10–15	12.82/20.31
LH	0–5/5–10	6.87/11.71	15–20/10–15	12.29/21.41
Arcuate nucleus	–/–	–/–	15–20/10–15	18.86/22.74
Posterior hypothalamus	5–10/5–10	7.88/11.03	–/–	–/–
Lateral parabrachial nucleus	5–10/5–10	6.73/9.24	–/–	–/–
Locus ceruleus	15–20/10–15	8.13/7.72	–/–	–/–
Raphe pallidus nucleus	5–10	6.58	10–15	11.13
Dorsal raphe nucleus	15–20	9.70	5–10	6.42
NTS	5–10/0–5	8.94/8.18	5–10/–	13.73/–
Zona incerta	–/5–10	–/13.99	5–10/10–15	9.14/8.13

–, not significant; left/right.

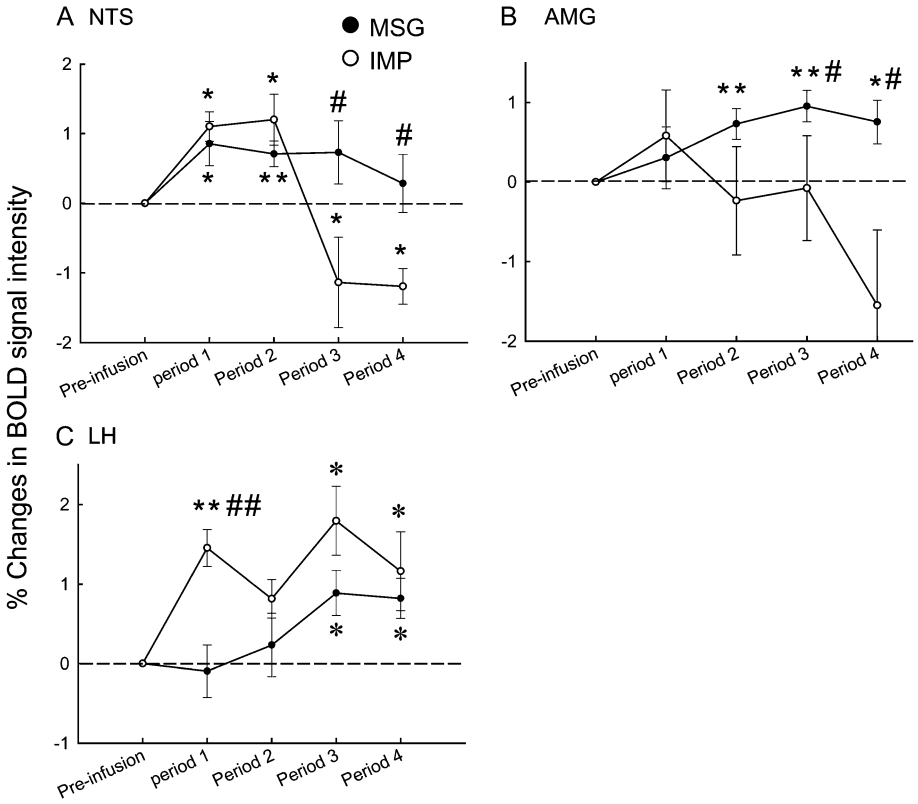

Figure 3 Time course of the BOLD signal changes in the NTS **(A)**, AMG **(B)**, and LH **(C)**. The BOLD signals were averaged every 5 min from the start of the infusion. Closed circle, MSG; open circle, IMP. Period 1, 0–5 min; period 2, 5–10 min; period 3, 10–15 min; period 4, 15–20 min. $^{*}P < 0.05$, $^{**}P < 0.01$, compared with the preinfusion period using paired *t*-test after analysis of variance. $^{\#}P < 0.05$, $^{\#\#}P < 0.01$, compared with IMP or MSG at the same period using paired *t*-test after analysis of variance.

decreased to the baseline level in the MSG group, it decreased significantly after the infusion was stopped in the IMP group. In the LH, the intragastric load of IMP induced a BOLD signal increase that occurred 0–5 min after the start of the infusion (period 1) and lasted until period 4. In the MSG group, the BOLD signal increased in period 3, and this increase lasted until period 4. In the AMG, the intragastric load of MSG induced a significant BOLD signal increase between period 2 and period 4 in the MSG group. We did not observe BOLD signal changes in the AMG for the IMP group.

Functional connectivity with BOLD changes in the NTS induced by intragastric loads of MSG or IMP

We used another technique to elucidate functional connectivity with regard to the NTS (Figure 4 and Table 2). In the MSG group, the BOLD signal changes in the raphe magnus nucleus, hippocampus, piriform cortex, AMG, medial preoptic area (mPOA), and insular cortex were correlated with those in the NTS. In the IMP group, the BOLD signal changes in the mediodorsal thalamus, hippocampus, piriform cortex, mPOA, septum, ventral orbital cortex, and insular cortex correlated with those in the NTS. In MSG group only, the BOLD signal changes in the raphe magnus nucleus, LH, AMG, and ventral pallidum correlated with those in the NTS, whereas in IMP group, the BOLD signal changes in the mediodorsal thalamus, septum, and ventral orbital cortex correlated with those in the NTS (Figure 4C,D and Table 2).

Discussion

In the present study, we demonstrated that intragastric loads of MSG and IMP induced BOLD signal changes in different brain regions. The time course of activation in several brain regions, including the NTS, LH, and AMG in MSG group differed from those in IMP group. These results were completely different from those obtained with intraoral chemoreception of Glu and IMP because both Glu and IMP interact with umami receptors in the oral cavity (Yasuo et al. 2008; Zhang et al. 2008), and both compounds are recognized as the same taste in the brain (de Araujo et al. 2003). We also used another analysis technique to demonstrate the brain regions displaying an activation that was correlated with that of the NTS. Together with the previous studies, these results

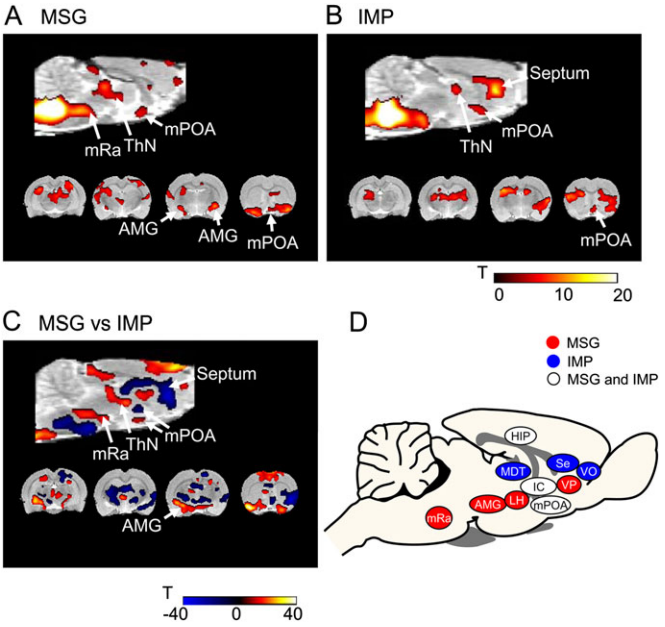

Figure 4 *T*-map images depicting the BOLD signals correlating with the BOLD signal changes in the NTS in **(A)** MSG and **(B)** IMP groups. **(C)** Comparisons of the BOLD signal intensity correlating with the BOLD signal changes in the NTS between MSG and IMP groups. *t* value shows the significant correlation of BOLD signals in MSG group compared with IMP group. Color bar, *t* value. **(D)** Schematic diagram of the brain regions associating with the activation in the NTS in MSG and IMP groups. Red areas are only MSG. Blue areas are only IMP. White areas are both MSG and IMP. MDT, mediodorsal thalamus; mRa, raphe magnus nucleus; Se, septum; VO, ventral orbital cortex; VP, ventral pallidum.

Table 2 Brain regions correlating with the BOLD increase in the NTS following the intragastric administration of an MSG or IMP solution ($P < 0.01$, corrected)

	MSG Maximum *t* value	IMP Maximum *t* value
Ventral orbital cortex	–/–	8.90/7.39
Insular cortex	6.05/–	6.04/–
Somatosensory cortex	8.72/8.03	–/10.34
Caudate putamen	–/5.24	9.62/6.7
Amygdala	6.99/11.19	–/–
Piriform cortex	6.3/7.24	–/6.55
Hippocampus	6.64/6.83	7.65/11.12
Septum	–/–	11.56/15.23
Ventral pallidum	7.00/9.64	–/–
Mediodorsal thalamus	–/–	7.20/7.80
Medial preoptic area	6.84/6.72	7.09/7.8
LH	8.11/–	–/–
Substantia nigra	6.50/7.26	–/–
Raphe pallidus nucleus	12.4	11.13
Raphe magnus nucleus	11.13	–

–, not significant; left/right.

indicate that Glu, and possibly IMP, activate regions of the brain through the vagus nerve. The sodium ion in the MSG group may contribute to this behavior. Our previous studies showed that intragastric administration of low concentrations of a NaCl solution had no effect on the BOLD response without caudate putamen (Tsurugizawa et al. 2008). Therefore, the BOLD response to an intragastric load of MSG is attributable to the Glu, not the sodium ion. In the present study, we selected the concentration of MSG and IMP as 60 and 30 mM. This is because these concentrations are the peak of the preference in rats (He et al. 2004). Although there were still possibilities that these differences in the activation patterns were due to the osmolarity and/or the calorie effect, our previous studies clearly showed that the forebrain activation by the Glu was not due to osmotic (Tsurugizawa et al. 2009). Intragastric infusion of isoosmotic (60 mM) NaCl and isocaloric (60 mM) glucose did evoke the different activation patterns from 60 mM MSG. Additionally, an intragastric infusion of 60 mM MSG also induces the conditioned flavored preference for the flavored water, which is paired with MSG. This effect is not induced by isocaloric glucose in rats, indicating that modulated preference by postingestive effect of MSG is not mainly by caloric effect (Uematsu et al. 2009). However, the possibility that some of the effects observed were due to differences in caloric content is still remained because 60 mM MSG and 30 mM IMP have different calories.

Although a previous study showed an increase in c-fos immunoreactivity to the intragastric infusion of MSG (Yamamoto and Sawa 2000), this approach was not temporally resolved. Some of the merits of using the fMRI technique in conscious rats are that we can investigate brain activity with temporal resolution throughout the entire brain (Stark et al. 2006) and that we can analyze the BOLD response in an awake state, same as humans and monkeys. Furthermore, using the time course data in each voxel, we can calculate the functional connectivity of various brain regions (Shyu et al. 2004; Schwarz et al. 2009). In the present study, we showed the distinct time course of BOLD signal changes in several brain regions, including the NTS and the LH. The results indicate that GI stimulation by MSG and IMP induces a BOLD response in the same brain regions but with distinct time courses. We also identified the distinct brain regions correlated with the NTS between the MSG and IMP groups.

Previously, our research showed that an intragastric load of MSG activated several brain regions, including the NTS, hypothalamus, and limbic system and that most of the brain activation was suppressed in totally or abdominally vagotomized rats, indicating that the abdominal vagus nerve is primarily responsible for mediating the MSG-induced brain activation (Uematsu et al. 2010). An electrophysiological

study also showed that vagal activity increases following an intragastric or enteric infusion of MSG (Niijima 2000). The vagus nerve terminates in the NTS and connects anatomically to the thalamus, hypothalamus, limbic system, and prefrontal cortex. Our data showed the possibility of a functional network between the NTS and several brain regions, including the raphe magnus nucleus, amygdala, hippocampus, mPOA, septum, insular cortex, and orbital cortex. These results are consistent with the c-fos studies showing that an intragastric load of MSG induces positive c-fos immunoreactivity in the NTS and the insular cortex (Yamamoto and Sawa 2000).

It was difficult to explain the difference in the BOLD responses between MSG and IMP stimulation because the peripheral afferent pathway that conveys the information about ingested IMP has been less well studied than that for MSG. One of the candidate pathways is a vagal pathway because the NTS, which is a terminal of the vagus nerve, was activated in the IMP group during the infusion period. Other researchers have also indicated that T1R receptors are present in the GI tract and could contribute to the chemoreception of Glu and IMP (Bezencon et al. 2007). Therefore, it is likely that the vagus nerve mediates the activation of the NTS following an intragastric load of IMP. An electrophysiological study revealed the role of the vagus nerve in the GI chemosensation of Glu, glucose, and NaCl in rats (Niijima 2000), but IMP has not yet been investigated. Humoral internal signals, for example, blood glucose, insulin, and other gut peptides, were not detected in both MSG and IMP (Viarouge et al. 1991). It is possible that an intragastric load of IMP could evoke humoral internal signals because IMP is an intermediate during the biosynthesis of purine nucleotides AMP and GMP (Moss et al. 1977). Further study of IMP in the GI tract is needed in the future.

In conclusion, we demonstrated that the intragastric administration of MSG and IMP induced distinct BOLD responses in several brain regions, including the NTS, thalamus, limbic system, and hypothalamic areas in conscious rats. These results indicate the existence of different mechanisms of chemosensing or metabolism in the GI tract for Glu and IMP. To clarify the mechanisms of the distinct brain activation patterns for these umami substances, further studies of GI chemoreception and hormonal secretion following GI administration of IMP are needed.

Acknowledgments

We are grateful to Mr Kuwazawa (Animal Support Kobe, Kobe, Japan) for technical assistance with the MRI measurements.

References

Bachmanov AA, Inoue M, Ji H, Murata Y, Tordoff MG, Beauchamp GK. 2009. Glutamate taste and appetite in laboratory mice: physiologic and genetic analyses. Am J Clin Nutr. 90:756S–763S.

Bezencon C, le Coutre J, Damak S. 2007. Taste-signaling proteins are coexpressed in solitary intestinal epithelial cells. Chem Senses. 32:41–49.

de Araujo IE, Kringelbach ML, Rolls ET, Hobden P. 2003. Representation of umami taste in the human brain. J Neurophysiol. 90:313–319.

He W, Yasumatsu K, Varadarajan V, Yamada A, Lem J, Ninomiya Y, Margolskee RF, Damak S. 2004. Umami taste responses are mediated by alpha-transducin and alpha-gustducin. J Neurosci. 24:7674–7680.

Moss J, Manganiello VC, Vaughan M. 1977. Substrate and effector specificity of a guanosine 3′:5′-monophosphate phosphodiesterase from rat liver. J Biol Chem. 252:5211–5215.

Nelson G, Chandrashekar J, Hoon MA, Feng L, Zhao G, Ryba NJ, Zuker CS. 2002. An amino-acid taste receptor. Nature. 416:199–202.

Niijima A. 1991. Effects of oral and intestinal stimulation with umami substance on gastric vagus activity. Physiol Behav. 49:1025–1028.

Niijima A. 2000. Reflex effects of oral, gastrointestinal and hepatoportal glutamate sensors on vagal nerve activity. J Nutr. 130:971S–973S.

Ninomiya Y, Nakashima K, Fukuda A, Nishino H, Sugimura T, Hino A, Danilova V, Hellekant G. 2000. Responses to umami substances in taste bud cells innervated by the chorda tympani and glossopharyngeal nerves. J Nutr. 130:950S–953S.

Paxinos G, Watson C. 1998. The rat brain in stereotaxic coordinates. 4th ed. San Diego (CA): Academic Press.

Ren X, Ferreira JG, Zhou L, Shammah-Lagnado SJ, Yeckel CW, de Araujo IE. 2010. Nutrient selection in the absence of taste receptor signaling. J Neurosci. 30:8012–8023.

Schwarz AJ, Gozzi A, Bifone A. 2009. Community structure in networks of functional connectivity: resolving functional organization in the rat brain with pharmacological MRI. Neuroimage. 47:302–311.

Shyu BC, Lin CY, Sun JJ, Chen SL, Chang C. 2004. BOLD response to direct thalamic stimulation reveals a functional connection between the medial thalamus and the anterior cingulate cortex in the rat. Magn Reson Med. 52:47–55.

Stark JA, Davies KE, Williams SR, Luckman SM. 2006. Functional magnetic resonance imaging and c-Fos mapping in rats following an anorectic dose of m-chlorophenylpiperazine. Neuroimage. 31:1228–1237.

Toyomasu Y, Mochiki E, Yanai M, Ogata K, Tabe Y, Ando H, Ohno T, Aihara R, Zai H, Kuwano H. 2010. Intragastric monosodium L-glutamate stimulates motility of upper gut via vagus nerve in conscious dogs. Am J Physiol Regul Integr Comp Physiol. 298:R1125–R1135.

Tsurugizawa T, Kondoh T, Torii K. 2008. Forebrain activation induced by postoral nutritive substances in rats. Neuroreport. 19:1111–1115.

Tsurugizawa T, Uematsu A, Nakamura E, Hasumura M, Hirota M, Kondoh T, Uneyama H, Torii K. 2009. Mechanisms of neural response to gastrointestinal nutritive stimuli: the gut-brain axis. Gastroenterology. 137:262–273.

Tsurugizawa T, Uematsu A, Uneyama H, Torii K. 2010. Effects of isoflurane and alpha-chloralose anesthesia on BOLD fMRI responses to ingested l-glutamate in rats. Neuroscience. 165:244–251.

Uematsu A, Tsurugizawa T, Kondoh T, Torii K. 2009. Conditioned flavor preference learning by intragastric administration of L-glutamate in rats. Neurosci Lett. 451:190–193.

Uematsu A, Tsurugizawa T, Uneyama H, Torii K. 2010. Brain-gut communication via vagus nerve modulate conditioned flavor preference. Eur J Neurosci. 31:1136–1143.

Viarouge C, Even P, Rougeot C, Nicolaidis S. 1991. Effects on metabolic and hormonal parameters of monosodium glutamate (umami taste) ingestion in the rat. Physiol Behav. 49:1013–1018.

Watterson SH, Chen P, Zhao Y, Gu HH, Dhar TG, Xiao Z, Ballentine SK, Shen Z, Fleener CA, Rouleau KA, et al. 2007. Acridone-based inhibitors of inosine 5′-monophosphate dehydrogenase: discovery and SAR leading to the identification of N-(2-(6-(4-ethylpiperazin-1-yl)pyridin-3-yl)propan-2-yl)-2-fluoro-9-oxo-9,10-dihydroacridine-3-carboxamide (BMS-566419). J Med Chem. 50:3730–3742.

Yamamoto T, Sawa K. 2000. c-Fos-like immunoreactivity in the brainstem following gastric loads of various chemical solutions in rats. Brain Res. 866:135–143.

Yamamoto T, Watanabe U, Fujimoto M, Sako N. 2009. Taste preference and nerve response to 5′-inosine monophosphate are enhanced by glutathione in mice. Chem Senses. 34:809–818.

Yasuo T, Kusuhara Y, Yasumatsu K, Ninomiya Y. 2008. Multiple receptor systems for glutamate detection in the taste organ. Biol Pharm Bull. 31:1833–1837.

Zhang F, Klebansky B, Fine RM, Xu H, Pronin A, Liu H, Tachdjian C, Li X. 2008. Molecular mechanism for the umami taste synergism. Proc Natl Acad Sci U S A. 105:20930–20934.